



ISSN: 0067-2904

## Mixed Spinel $Co_{0.4}Zn_{0.6}Fe_2O_4$ Ferrite Nanoparticles As a Magnetic Photocatalyst: Synthesis and Dye Degradation

We'am Sami

Department of Physics, College of Education, University of Al-Qadisiyah, Qadisiyah, Iraq.

Received: 12/7/2021

Accepted: 24/8/2022

Published: 30/3/2023

### Abstract

In this paper, mixed spinel  $Co_{0.4}Zn_{0.6}Fe_2O_4$  ferrite was synthesized by microwave-assisted combustion method. Photocatalytic activity of the as-synthesized sample was investigated against methylene blue dye at room temperature at different exposure times (60-360 min.) under visible light. Phase impurity and surface morphology which are investigated with XRD analysis and field emission- scanning electron microscopy, indicate that a cubic spinel unit cell structure with a crystallite size and lattice constant are 22.5048nm and 8.37Å, respectively. The saturation magnetization exhibited directly from the hysteresis loop is (70.20emu/g). Optical properties for the investigated ferrites exhibited photo absorption from UV to visible region with an energy gap of (1.6 eV). Mainly two broad metal-oxygen bands for spinel  $Co_{0.4}Zn_{0.6}Fe_2O_4$  ferrite photocatalyst are seen in FT-IR spectra. The degradation ratio of dye increased as exposure time was increased.

**Keywords:** Ferrites, glycine, combustion route, photocatalyst, magnetic properties

## فرايت المختلط النانوية كمحفز ضوئي مغناطيسي: التصنيع $Co_{0.4}Zn_{0.6}Fe_2O_4$ جسيمات السبيل وانحلال الصبغة

وئام سامي

قسم الفيزياء, كلية التربية, جامعة القادسية, القادسية, العراق

### الخلاصة

في هذا البحث تم تصنيع  $Co_{0.4}Zn_{0.6}Fe_2O_4$  سبيل فرايت المختلط باستخدام طريق الاحتراق بمساعدة الميكروويف. تم دراسة قابلية التحفيز الضوئي لانحلال صبغة المثلين الزرقاء من المياه العادمة في درجة حرارة الغرفة بازمان تعريض مختلفة (60-360) دقيقة بوجود الضوء المرئي. أظهرت نقاوة الطور وتشكلات السطح التي تم فحصها بتحليل XRD والمجهر الإلكتروني الماسح للانبعثات إلى شكل بنية الإسبنيل بحجم بلوري وثابت شبكيه (22,5048 نانومتر) و (8,37 كستروم) على التوالي. وجدت قيم مغنطة التشبع (70,20) وحدة كهرومغناطيسية / غرام مباشرة من حلقة الهستره. أظهرت الخواص البصرية للفريتات التي تم فحصها امتصاصاً ضوئياً من الأشعة فوق البنفسجية إلى المنطقة المرئية مع فجوة طاقة (1,6) إلكترون فولت. بين طيف FT-IR ان هناك نطاقتان عريضتان من الفلز - اوكسجين المحفز الضوئي فرايت كوبلت خارصين. كما ان انحلال الصبغة يزداد عند زيادة زمن التعريض.

\* Email: [weam.sami@qu.edu.iq](mailto:weam.sami@qu.edu.iq)

## 1. Introduction

Photocatalysis for water treatments is a modern technology used to purify water. Many processes, including extraction, polymerization, and photocatalytic degradation, have been developed to reduce organic toxicity in water. Photocatalysis can be described as an acceleration of a photo-induced reaction using catalysts [1]. Magnetic catalysts' properties have opened a new area in separation applications. Iron-based nanoparticles have been extensively studied[2]. Ferrites are compounds of mixed oxides of iron and one or more other materials with ferromagnetic properties. Based on their crystal structures, ferrites can be categorized into three groups: spinel, garnet and hexagonal, each having its own importance [3,4]. When a photocatalyst is selected, The material's band gap determines the wavelength of light that it absorbs. Ferrites offer the advantage of having a band gap capable of absorbing visible light[5]. The adsorption and degradation processes using spinel ferrite based nanomaterials play an important role in the removal of harmful dyes, phenols and traces of toxic metals from the water [6]. Ferrite catalysts' capability is possible because of the effective utilization of light energy, which enables the formation of  $e^-/h^+$  pairs on the photocatalytic surface.  $e^-/h^+$  pairs, due to their resistance to oxidation and reduction, play an important role in the formation of reactive oxygen compounds, such as  $\cdot\text{OH}$  and  $\text{O}_2^{\cdot-}$ , thereby facilitating pollutant decomposition[7]. Earlier studies have shown that the magnetic properties could be changed by adding other metal atoms[8]. Various techniques, such as co-precipitation[9], ceramic processing[8] and sol-gel method [10], were used to synthesize these kinds of ferrites. The solution combustion route is widely used to prepare single or mixed metal oxides. To increase the efficiency of the nitrate combustion synthesis route, organic compounds such as urea, glycine, carbohydrazide, or citric acid have been added with metal. Metal nitrates act as oxidants and as sources of cations, and the organic compound acts as fuel [11]. In the present work, mixed spinel  $\text{Co}_{0.4}\text{Zn}_{0.6}\text{Fe}_2\text{O}_4$  ferrite powder was synthesized with a microwave-assisted combustion route, using glycine as a fuel; their physical and magnetic properties were examined.

## 2. Materials and Methods

### 2.1. Synthesis of Mixed Spinel $\text{Co}_{0.4}\text{Zn}_{0.6}\text{Fe}_2\text{O}_4$ Ferrite Photocatalyst

High purity nitrate salts of (Cobalt- Zinc: Iron) [99% from HIMEDIA Co., India] were the raw materials with a molar ratio 1:2 for Co-Zn: Fe. Each material was weighed separately in stoichiometric ratio and dissolved in a suitable quantity of distilled water. The solution was mixed and stirred for 20 minutes. Stoichiometrically amount of fuel (glycine) with the chemical formula ( $\text{C}_2\text{H}_5\text{NO}_2$ ) [Glycine to nitrate ratio 0.33] was added into the mixture. The mixture after 20 minutes was transferred to a microwave oven with microwave irradiation power of 800 Watt. The solution boiled and started releasing many gases such as  $\text{CO}_2$ ,  $\text{NO}_2$ , and  $\text{N}_2$  after dehydration accompanied by decomposition. As the solution reached the point of spontaneous combustion, it started to burn and release heat, causing the solution to vaporize and become solid. The product powder was washed with ethanol and distilled water three times and dried at (70 °C) for 2 hours. The resulting powder was ground for 2 minutes with a mortar to obtain fine powder. These preparation steps are shown in Figure 1.

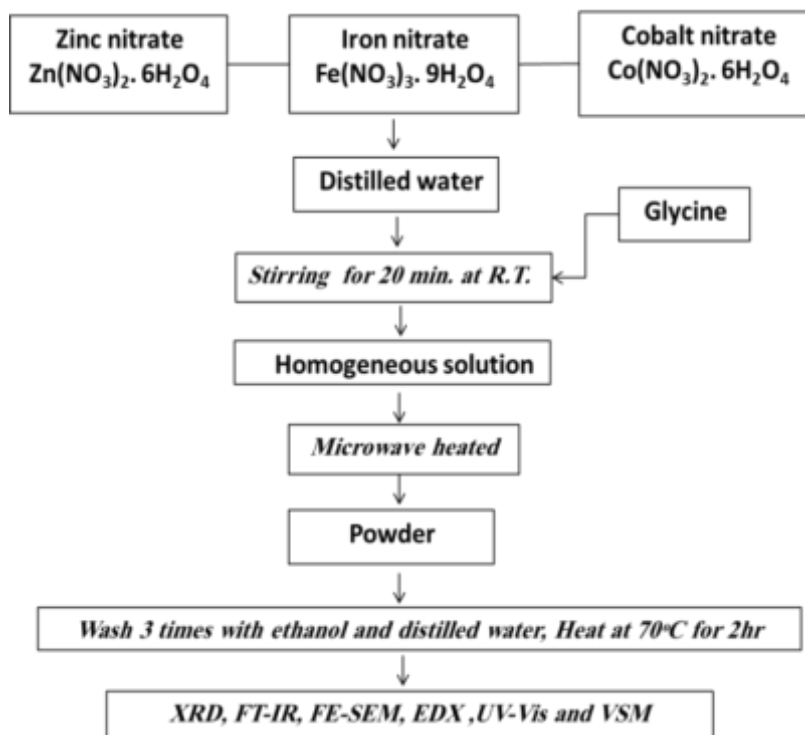


**Figure 1:** A schematic representation of microwave-assisted combustion route used for mixed spinel  $\text{Co}_{0.4}\text{Zn}_{0.6}\text{Fe}_2\text{O}_4$  ferrite photocatalyst.

The XRD patterns of the as-synthesized powdered mixed spinel  $\text{Co}_{0.4}\text{Zn}_{0.6}\text{Fe}_2\text{O}_4$  ferrite photocatalyst were recorded with an X-ray diffractometer (Shimadzu, model XRD 6000), the FE-SEM images and EDS analysis were obtained with a scanning electron microscope (FEI Nova Nano SEM 450), and the optical properties were studied with a UV-Visible scanning spectrophotometer ((Shimadzu-8400S spectrometer, Shimadzu-UV1800).

## 2.2. Photocatalytic Activity

The photocatalytic activity was carried out via methylene blue (MB) dye with a concentration of (5gm/l). The pH value was controlled using NaOH. Source light was placed horizontally on the beaker containing a mixture of 40 ml of MB dye and water solution and (0.10g) of catalyst with stirring. After the adsorption process was completed, the catalyst was separated from the solution using a magnet bar. At this stage, (3ml) of the sample was taken and was analyzed to determine the absorbance with a UV-Vis spectrophotometer. The photocatalytic activity was determined at various exposure times (60-360min.). The degradation efficiency (D) can be calculated by the following equation[1]:

$$D\% = \frac{A_0 - A}{A} \times 100 \quad \text{..... (1)}$$

Where absorbance at zero exposure time ( $t_0$ ) and absorbance at ( $t$ ) exposure time are ( $A_0$ ) and ( $A$ ), respectively. It is possible to explain the degradation kinetics ( $k$ ) of the MB dye using the first-order Langmuir equation represented by [12]:

$$\frac{1}{C_t} = \frac{1}{C_0} + kt \quad \text{..... (2)}$$

Where ( $C_0$ ) and ( $C_t$ ) are the initial concentration and concentration after light exposure, respectively.

### 3. Results and Discussion

#### 3.1. Structure and Impurity Phases Characterization

XRD pattern for the as-synthesized powdered mixed spinel  $\text{Co}_{0.4}\text{Zn}_{0.6}\text{Fe}_2\text{O}_4$  ferrite photocatalyst is displayed in Figure 2. The peaks could be easily indexed as (220), (311), (222), (400), (422), (511), and (440). All the planes are allowed planes, which indicate the formation of cubic spinel structure with the lattice constant ( $8.37 \text{ \AA}$ ) following the standard (JCPDS card No. 00.22-1012) for Zn-ferrite and (JCPDS card no.00- 22-1086 ) for Co-ferrite. Peaks of the impurity phase (CoO) (indicated by \*) were observed in the XRD pattern. The diffraction peaks were broad, sharp and narrow; this indicates a decrease in the particle size.

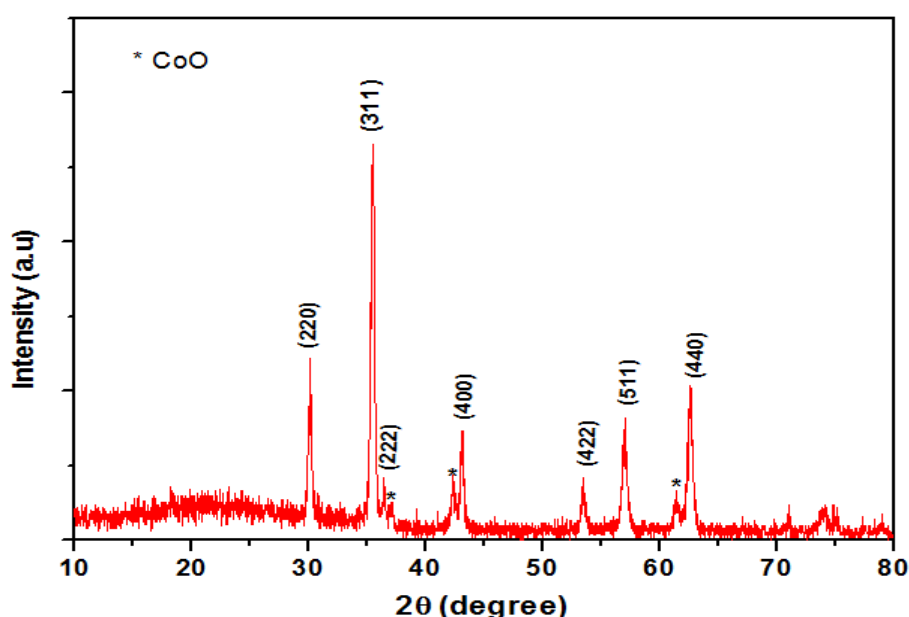


**Figure 2:** XRD pattern for as-synthesized powdered mixed spinel  $\text{Co}_{0.4}\text{Zn}_{0.6}\text{Fe}_2\text{O}_4$  ferrite photocatalyst

From the highest intensity peak in the XRD spectrum, the (311) plane, and depending on the Scherrer's equation[12] and Bragg's law[13], the structure parameters such as crystallite size ( $D$ ) and lattice constant were determined as shown in Table 1.

**Table 1:** Structure parameters for as-synthesized powdered mixed spinel  $\text{Co}_{0.4}\text{Zn}_{0.6}\text{Fe}_2\text{O}_4$  ferrite photocatalyst

photocatalyst	$2\theta$ (deg)	FWHM (deg)	Lattice Constant $a$ ( $\text{\AA}$ )	Crystallite Size (XRD) $D$ (nm)
$\text{Co}_{0.4}\text{Zn}_{0.6}\text{Fe}_2\text{O}_4$	35.5255	0.34960	8.37	22.5048

From Table 1, it is clear that the crystallite size (DXRD) confirms that the mixed spinel  $\text{Co}_{0.4}\text{Zn}_{0.6}\text{Fe}_2\text{O}_4$  ferrite is in the nanoscale.

### 3.2. Morphological and Chemical Composition Analysis

In Figure 2, the FE-SEM images and EDS analysis for as-synthesized powdered mixed spinel  $\text{Co}_{0.4}\text{Zn}_{0.6}\text{Fe}_2\text{O}_4$  ferrite photocatalyst are given.

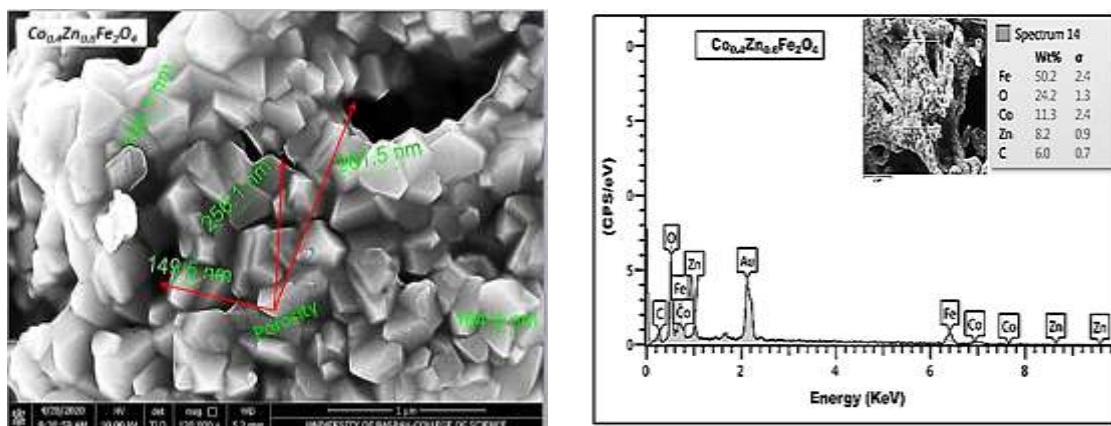


**Figure 3:** FE-SEM images and EDS analysis for as-synthesized powdered mixed spinel  $\text{Co}_{0.4}\text{Zn}_{0.6}\text{Fe}_2\text{O}_4$  ferrite photocatalyst.

FE-SEM images showed agglomerated, uniformly distributed particles with porosity. Compared between this investigation and other reported [14-16], agglomeration may be due to van der Waals forces between the nanoparticles or by organic compounds exhibited in the samples. Furthermore, particles in the nanoscale have a large surface area-to-volume ratio and very high surface energy. To reduce this high surface energy, the particles in the nanoscale tend to agglomerate. EDS analysis for the as-synthesized powdered mixed spinel  $\text{Co}_{0.4}\text{Zn}_{0.6}\text{Fe}_2\text{O}_4$  ferrite photocatalyst indicated that the basic compositions of regular samples are Co, Zn, Fe and O. The presence of C was from the black carbon tape used.

### 3.3. Fourier Transforms - Infrared (FT-IR) Spectroscopy Characterization

The FTIR spectrum for the as-synthesized powdered mixed spinel  $\text{Co}_{0.4}\text{Zn}_{0.6}\text{Fe}_2\text{O}_4$  ferrite photocatalyst was recorded at the range of  $(4000 - 450 \text{ cm}^{-1})$  (as pellets in KBr) and as depicted in Figure 4.

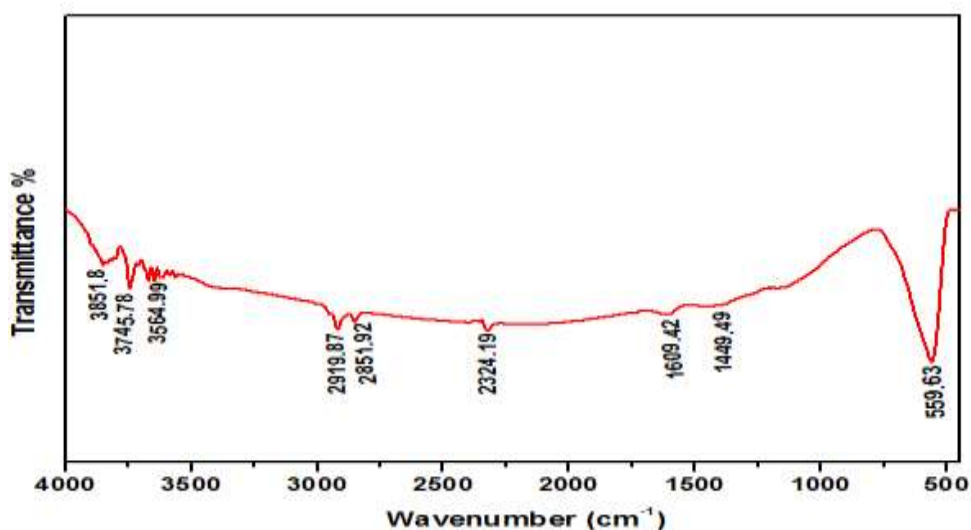


**Figure 4:** FT-IR spectra for as-synthesized powdered mixed spinel  $\text{Co}_{0.4}\text{Zn}_{0.6}\text{Fe}_2\text{O}_4$  ferrite photocatalyst.

Broad metal-oxygen bands are seen in the spectrum, and ferrites, in particular, are typically observed in the range  $600\text{--}500\text{cm}^{-1}$ . The peaks at ( $\sim 1374\text{ cm}^{-1}$ ) are referred to H–O–H bending vibration in  $\text{H}_2\text{O}$  or OH deformation vibration because of surface hydroxyls; those imply excellent hydrophobicity suitable to the photocatalytic activity of ferrites. However, in the present search peaks at  $559.63$  indicating the formation of spinel ferrite structure are present in the spectrum. The aforementioned peak also confirmed the formation of tetrahedral structures. Similar results were observed in other studies [17 - 19].

### 3.4. Optical properties

The absorption spectrum for the as-synthesized powdered mixed spinel  $\text{Co}_{0.4}\text{Zn}_{0.6}\text{Fe}_2\text{O}_4$  ferrite photocatalyst as a function of wavelength is shown in Figure 5.

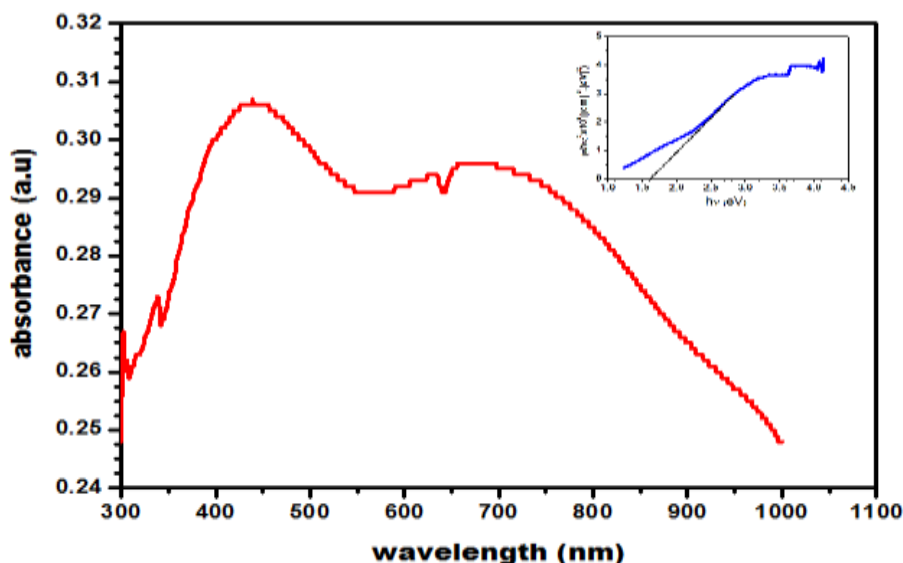


**Figure 5:** Absorption as a function of wavelength for as-synthesized powdered mixed spinel  $\text{Co}_{0.4}\text{Zn}_{0.6}\text{Fe}_2\text{O}_4$  ferrite photocatalyst (insert shows energy gap plot).

In this spectrum, mixed spinel  $\text{Co}_{0.4}\text{Zn}_{0.6}\text{Fe}_2\text{O}_4$  ferrite photocatalyst demonstrated extended photo absorption from UV to the visible region. This is compatible with the previous work suggested by Tatarchuk et al. [20]. To estimate the optical band gap for samples, the Tauc-relation is commonly used. The estimation of the band gap energy from  $(\alpha h\nu)^2$  as a function of the incident energy ( $h\nu$ ) plot is inserted in Figure 5. The optical gap is the intercept of the linear part extrapolation to the Y-axis. Mixed spinel  $\text{Co}_{0.4}\text{Zn}_{0.6}\text{Fe}_2\text{O}_4$  ferrite band gap energy was recorded at  $1.6\text{ eV}$ . This energy gap value was in very good agreement with that reported by Tatarchuk of  $1.59\text{ eV}$  [20].

### 3.5. Magnetic Measurements

The magnetic measurements for the as-synthesized powdered mixed spinel  $\text{Co}_{0.4}\text{Zn}_{0.6}\text{Fe}_2\text{O}_4$  ferrite photocatalyst were carried out with an applied field of (15KOE). In Figure 6, the hysteresis loop for the as-synthesized powdered mixed spinel  $\text{Co}_{0.4}\text{Zn}_{0.6}\text{Fe}_2\text{O}_4$  ferrite photocatalyst has a high value of coercivity with values of saturation magnetization of ( $70.20\text{ emu/g}$ ).

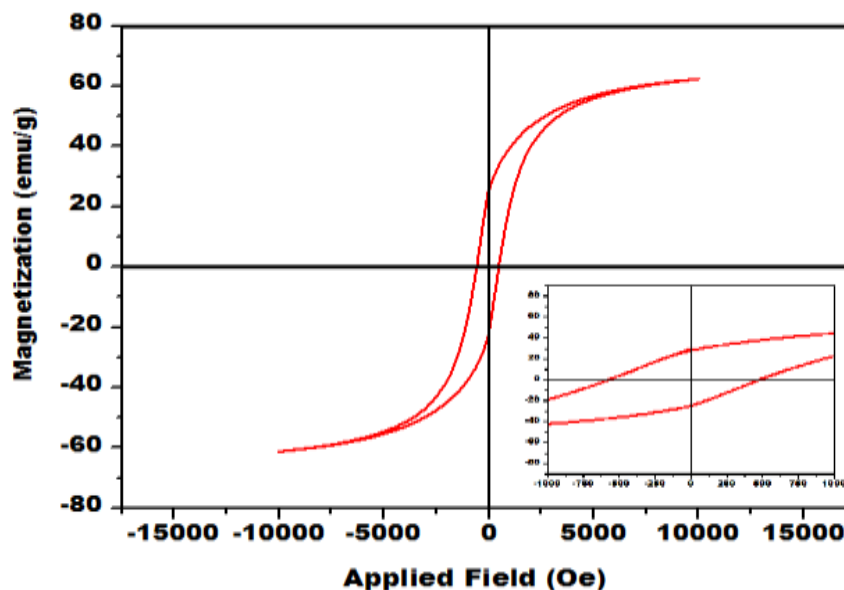


**Figure 6:** Magnetic hysteresis loop for as-synthesized powdered mixed spinel  $\text{Co}_{0.4}\text{Zn}_{0.6}\text{Fe}_2\text{O}_4$  ferrite photocatalyst [coercivity plot insert]

The values of the magnetic parameters such as remanence magnetization ( $M_r$ ), saturation magnetization ( $M_s$ ), coercivity ( $H_c$ ) and squareness ratio ( $M_r/M_s$ ) of the as-synthesized powdered mixed spinel  $\text{Co}_{0.4}\text{Zn}_{0.6}\text{Fe}_2\text{O}_4$  ferrite were directly extracted from this curve and are listed in Table 2.

**Table 2 :** Magnetic measurements extracted from hysteresis loops for as-synthesized powdered mixed spinel  $\text{Co}_{0.4}\text{Zn}_{0.6}\text{Fe}_2\text{O}_4$  ferrite photocatalyst .

photocatalyst	Saturation Magnetization $M_s$ (emu/g)	Remanence Magnetization $M_r$ (emu/g)	coercivity $H_c$ (Oe)	squareness ratio $M_r/M_s$
$\text{Co}_{0.4}\text{Zn}_{0.6}\text{Fe}_2\text{O}_4$	70.20	25	500	0.35

From Table 2, the coercivity for these samples was found to be (500) Oe. To explain the effect of reducing domain, the squareness ratio ( $M_r/M_s$ ) was calculated for each sample. A squareness ratio of about 0.5 means that a single magnetic domain sample has been produced[21]. From Table 2, it is clear that as-synthesized powdered mixed spinel  $\text{Co}_{0.4}\text{Zn}_{0.6}\text{Fe}_2\text{O}_4$  ferrite photocatalyst has single domain structures.

#### 4. Dye Degradation

Figure 7 shows the absorbance spectra of MB dye measured with various exposure times (60–360 min). The absorbance of MB dye decreases with the increase of irradiation time. This result indicates increase in the degradation efficiency of the photocatalysts. Figure 8 shows the calibration plot of MB dye at a wavelength of 664 nm. Degradation rate (%) and  $k$  value with irradiation time are shown in Figures 9 and 10, the obtained values are listed in Table 3. Figure 9 shows the relationship between the degradation rate of MB dye and irradiation time. Notably, degradation efficiency increases with irradiation time in the MB dyes. Figure 10 shows  $C/C_0$  plot versus the irradiation time for the as-synthesized powdered mixed spinel  $\text{Co}_{0.4}\text{Zn}_{0.6}\text{Fe}_2\text{O}_4$  ferrite photocatalyst for MB dyes with various exposure times; the concentration of the MB dye decreases with the increase of irradiation time.



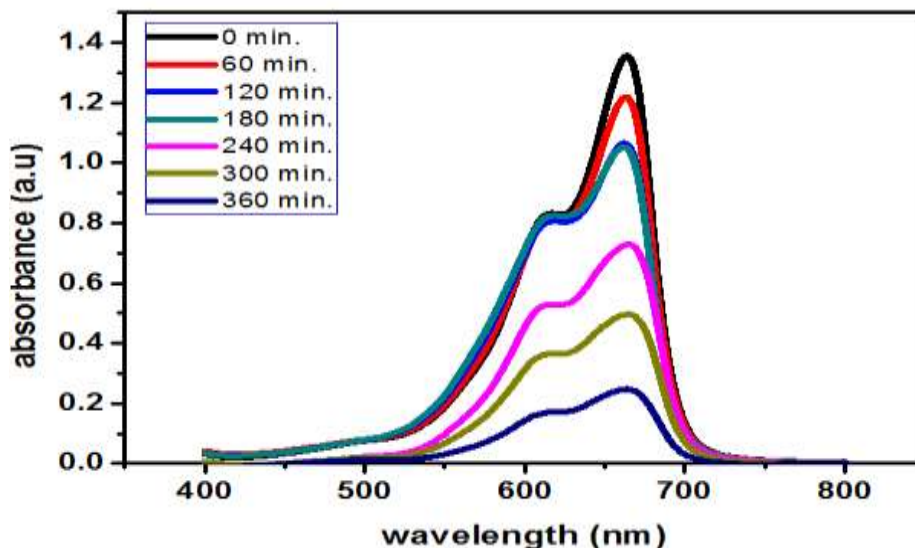


**Figure 7:** UV-Vis spectra of MB dye photocatalytic at different visible light exposure times.

**Table 3:** The obtained values of the degradation rate (%) and reaction rate constant (K) with different irradiation times for as-synthesized powdered mixed spinel  $\text{Co}_{0.4}\text{Zn}_{0.6}\text{Fe}_2\text{O}_4$  ferrite photocatalyst

photocatalyst	PH	D%						K ( $\text{min}^{-1}$ )
		60 min	120 min	180 min	240 min	300 min	360 min	
$\text{Co}_{0.4}\text{Zn}_{0.6}\text{Fe}_2\text{O}_4$	11	10.16	21.73	22.69	46.49	63.37	81.94	0.0046

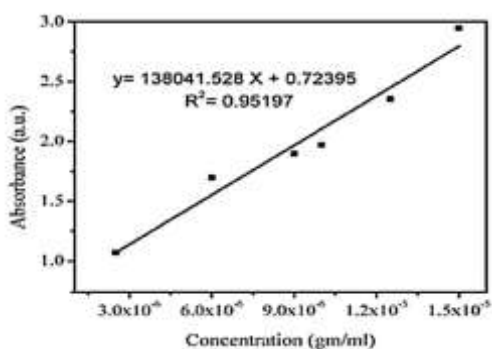


**Figure 8:** standard calibration curve of (MB) at 664 nm[1].

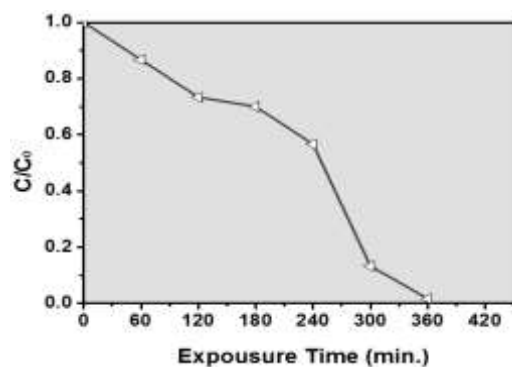


**Figure 9:** Kinetics of photocatalytic degradation with various exposure times



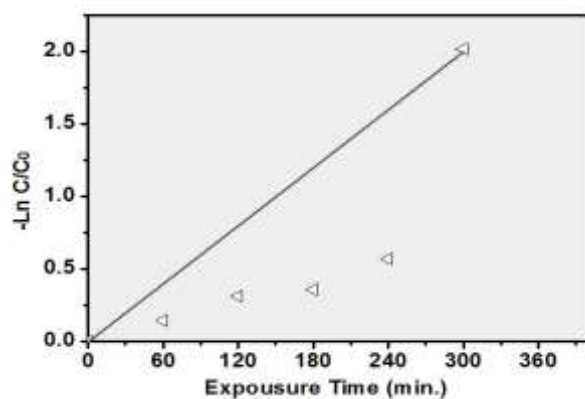


**Figure 10:** Variation of  $-\ln(C/C_0)$  with different

## 5. Conclusion

In summary, mixed spinel  $\text{Co}_{0.4}\text{Zn}_{0.6}\text{Fe}_2\text{O}_4$  ferrite photocatalyst was successfully synthesized using a microwave-assisted combustion route. It is a facile, short-time and environmentally friendly method that provides high-yield nanosized ferrite via well crystalline structure, uniform particle sizes, and good magnetic properties. The results show that the degradation rate of MB increased from [10.16-81.94] when irradiation time increased from [60-360min.].

## Acknowledgment

The author is grateful to the University of Baghdad, Iraq, University of Mashhad, Iran and University of Basrah, Iraq for providing characterizations facilities for the present work.

## References

- [1] M.J. Kadhim, M.A. Mahdi, and J.J. Hassan, "Influence of pH on the Photocatalytic Activity of ZnO Nanorods," *Material Internationals*, vol. 2, no. 2 pp. 0064 - 0072, 2020. <https://doi.org/10.33263/Materials21.064072>.
- [2] N. M. Mahmoodi, "Zinc Ferrite Nanoparticle as a Magnetic Catalyst: Synthesis and Dye Degradation," *Materials Research Bulletin*, vol. 48, no. 10, pp. 4255–4260, 2013. <http://dx.doi.org/10.1016/j.materresbull.2013.06.070>.
- [3] W. Sami, Z.S. Sadeq, "Synthesis, Characterizations, and Magnetic Properties of Mixed Spinel  $\text{Mg}_{1-x}\text{Zn}_x\text{Fe}_2\text{O}_4$  Ferrites," *Iraqi J. Sci.*, vol. 63, no. 3, pp. 997-1003, 2022. <https://doi.org/10.24996/ij.s.2022.63.3.9>
- [4] W. Sami, Z. S. Sadeq, "Role of Glycine-to-Nitrate Ratio in Physical and Magnetic Properties of Zn-Ferrite Powder," *Iraqi J. Sci.*, vol. 63, no. 1, pp. 170-181, 2022. <https://doi.org/10.24996/ij.s.2022.63.1.18>
- [5] E. Casbeer, V. K. Sharma and X-Z Li, "Synthesis and Photocatalytic Activity of Ferrites Under Visible Light," A review in *Separation and Purification Technology*, vol. 87, pp. 1–14, 2012. <https://doi.org/10.1016/j.seppur.2011.11.034>
- [6] D. Chahar, S. Taneja, S. Bisht, S. Kesarwani, P. Thakur, A. Thakur, P. B. Sharma, "Photocatalytic Activity of Cobalt Substituted Zinc Ferrite for The Degradation of Methylene Blue Dye Under Visible Light Irradiation, *Journal of Alloys and Compounds*," vol. 851, pp. 1-9, 2021. <https://doi.org/10.1016/j.jallcom.2020.156878>
- [7] L. T. T. Nguyen, L. T. H. Nguyen, N. C. Manh, D. N. Quoc, H. N. Quang, H. T. T. Nguyen, D. C. Nguyen and L. G. Bach, "A Facile Synthesis, Characterization, and Photocatalytic Activity of Magnesium Ferrite Nanoparticles via the Solution Combustion Method," *Research Article in Journal of Chemistry*, vol. 2019, pp. 1-8, 2019. <https://doi.org/10.1155/2019/3428681>
- [8] A. Hassadee, T. Jutarosaga and W. Onreabroy, "Effect of Zinc Substitution on Structural and Magnetic Properties of Cobalt Ferrite," *Procedia Engineering*, vol. 32, pp. 597 – 602, 2012. <https://doi.org/10.1016/j.proeng.2012.01.1314>

- [9] S. N. Dolia, A. S. Prasad, M. S. Dhawan, S. Chander and M. P. Sharma, "Mössbauer Study of Nanoparticles of  $\text{Co}_{0.4}\text{Zn}_{0.6}\text{Fe}_2\text{O}_4$ ," *Indian journal of pure & Applied Physics*, vol. 45, no. 10, pp. 826-829, 2007.
- [10] I. A. Amar, S. I. Faraj, M. A. Abdulqadir, I. A. Abdalsamed, F. A. Altohami, and M. A. Samba, "Oil Spill Removal from Water Surfaces Using Zinc Ferrite Magnetic Nanoparticles As a Sorbent Material," *Iraqi J. Sci*, vol.62, no.3, pp. 718-728, 2021. <https://doi.org/10.24996/ij.s.2021.62.3.2>
- [11] M. R. de Freitas , G. L. de Gouveia , L. J. D. Costa , A. J. A. de Oliveira and R. H. G. A. Kiminami," Microwave Assisted Combustion Synthesis and Characterization of Nanocrystalline Nickel-doped Cobalt Ferrites," *Materials Research*, vol. 19, no. 4 , pp. 27-32, 2016. <https://doi.org/10.1590/1980-5373-MR-2016-0077>
- [12] M. Sundararajan, L. J. Kennedy, P. Nithya, J.J. Vijaya and M. Bououdina, "Visible Light Driven Photocatalytic Degradation of Rhodamine B using Mg Doped Cobalt Ferrite Spinel Nanoparticles Synthesized by Microwave Combustion Method," *Journal of Physics and Chemistry of Solids*, vol.108, pp. 61-75, 2017. <http://dx.doi.org/10.1016/j.jpics.2017.04.002>.
- [13] B. B. V. S. V Prasad, K. V. Ramesh and A. Srinivas," Structural and Magnetic Studies of Nano-Crystalline Ferrites  $\text{MFe}_2\text{O}_4$  (M =Zn, Ni, Cu, and Co) Synthesized Via Citrate Gel Auto Combustion Method," *J Supercond Nov Magn.*,vol. 30, pp. 3523–3535, 2017. DOI:10. 1007 /s 10948-017-4153-y
- [14] A. T. Dhiwahara, M. Sundararajan, P.Sakthivel, C. S. Dashd and S. Yuvaraj. "Microwave-Assisted Combustion Synthesis of Pure and Zinc-Doped Copper Ferrite Nanoparticles: Structural, Morphological, Optical, Vibrational, and Magnetic Behavior," *Journal of Physics and Chemistry of Solids*, vol.138,pp.1-36, 2020 . <https://doi.org/10.1016/j.jpics.2019.109257>
- [15] P. Tehrani, A. Shokuhfar and H. Bakhshi, "Tuning the Magnetic Properties of  $\text{ZnFe}_2\text{O}_4$  Nanoparticles Through Partial Doping and Annealing," *Journal of Superconductivity and Novel Magnetism*, vol. 32, pp. 1013-1025, 2018. Doi.org/10.1007/s10948-018-4785-6.
- [16] P. A. Udhaya, M. Meena and M. A. J. Queen, "Green Synthesis of  $\text{MgFe}_2\text{O}_4$  Nanoparticles Using Albumen as Fuel and their Physico-Chemical Properties," *International Journal of Scientific Research in Physics and Applied Sciences*, vol. 7, no. 2, pp. 71-74, 2019. <https://doi.org/10.26438/ijrpsas/v7i2.7174>.
- [17] T. M. Hammad, J. K. Salem, A. A. Amsha and N K. Hejazy, "Optical and Magnetic Characterizations of Zinc Substituted Copper Ferrite Synthesized by a Co-Precipitation Chemical Method," *Journal of Alloys and Compounds*, vol. 741, pp. 123-130, 2018 . <https://doi.org/10.1016/j.jallcom.2018.01.123>.
- [18] M. Shahid, L. Jingling , Z. Ali, I. Shakir , M. F. Warsi, R.Parveen and M. Nadeem, "Photocatalytic Degradation of Methylene Blue on Magnetically Separable  $\text{MgFe}_2\text{O}_4$  Under Visible Light Irradiation," *Materials Chemistry and Physics*, vol. 139, pp. 566-571, 2013. <http://dx.doi.org/10.1016/j.matchemphys.2013.01.058>
- [19] K. J. Jameel , S. Mohamed, and A. Sh. Mahmoud, "Studying the Structural Properties of Mg-Zn Ferrite Nano Particle Prepared by Auto Combustion Sol-gel Method," *Tikrit Journal of Pure Science* ,vol. 21, pp. 63-67,2016.
- [20] T.R. Tatarchuk, N.D. Paliychuk, M. Bououdina, B. Al-Najar, M. Pacia, W. Macyk, and A. Shyichukd, "Effect of Cobalt Substitution on Structural, Elastic, Magnetic and Optical Properties of Zinc Ferrite Nanoparticles," *Journal of Alloys and Compounds*, vol. 731, pp. 1256-1266, 2018. <https://doi.org/10.1016/j.jallcom.2017.10.103>.
- [21] V. Badwaik, D. Badwaik , V. Nanoti and K. Rewatkar,"Study of Some Structural and Magnetic Properties of  $\text{Sr}_2\text{Me}_2\text{Fe}_{11}(\text{SnCo})_{0.5}\text{O}_{22}$  NanoFerrites," *International Journal of Knowledge Engineering*, vol.3, no. 1, pp. 58-60, 2012